Density-Based Classification and Iron Content Estimation of the Bloomery Iron Semi-Products: An Experimental Approach to Post-Reduction Technological Characterization

Vasbucák kategorizálása és vastartalmuk becslése a sűrűségük alapján - próbakohósítások eredményeképpen kapott vasbucák vastömbé kovácsolása

Ádam Thiele
Department of Materials Science and Engineering,
Faculty of Mechanical Engineering,
Budapest University of Technology and Economics,
Műegyetem rkp. 3.,
H-1111 Budapest,
Hungary
thiele.adam@gmail.com – corresponding author

Tena Karavidović
Institute of Archaeology,
Jurjevska ulica 15,
10 000 Zagreb
Croatia
tkaravidovic@iarh.hr

Abstract
The study presents a framework for estimating metallic iron content and the degree of refinement in archaeological iron semi-products using non-destructive bulk density measurement. Visual inspection, simple metrics and conventional structural analysis reveal aspects of bloomery technology but seldom yield comparable quantitative indicators of technological practice. Moreover, structural analysis frequently includes invasive sectioning. To address this limitation, changes in semi-product density during post-reduction refining—from iron sponge to purified bars—were evaluated through a programme of experimental refining, density measurement, structural analysis and predictive modelling. On this basis, a four-stage typology with indicative density ranges for 1-5 kg heavy blooms is proposed: (1) uncompacted sponge, 3–4 g/cm³; (2) compacted bloom, 3,5–5 g/cm³; (3) reheated/consolidated bloom, 5–6 g/cm³; and (4) purified bars with slag inclusions - 7,3-7,7 g/cm³. A linear relation between bulk density (ρ) and metallic iron content (Fe%) was derived (Fe% ≈ 9.24ρ + 27,2), permitting estimation of metallic iron content and mass of a semi-product at any given density. The framework standardises technological characterisation of iron production stages and supports comparative analysis across diverse archaeological contexts through a replicable, scalable protocol linking experimental archaeology with morphology-based artefact analysis.

Keywords: iron sponge, iron bloom, iron bar, smithing, archaeometallurgy
Kulcsszavak: Vasszivacs, vasbuca, vastömb, vastartalom, kovácsolás, acheometallurgia

1. Introduction
In the context of pre-industrial metallurgy, the production of iron involved a complex *chaîne opératoire* centred on the direct reduction of iron ore and subsequent post-reduction processing (Pleiner 2000; Buchwald 2005). This multi-stage technological system can be broadly divided into two principal phases: smelting and smithing. Direct reduction smelting is a solid-state chemical process in which iron ore is reduced to metallic iron by exposure to a carbon-rich, reducing atmosphere, typically at temperatures between 1,100 and 1,300 °C. This is conducted in a bloomery furnace—usually a shaft or bowl-type structure made traditionally of clay or stone materials. While furnace design and geometry vary across archaeological periods and cultural regions, the process operates within broadly consistent parameters. During smelting, iron oxides are reduced by carbon monoxide (generated through charcoal combustion), producing a spongy mass of metallic iron interspersed with slag and other impurities—referred to as an iron bloom. Following extraction from the furnace, the raw iron bloom must undergo mechanical and thermal refinement to reduce impurity level (slag content) and porosity and make it usable for further processing into objects. This stage, broadly referred to as post-reduction, can theoretically consists of two or three successive phases: 1) Compaction – directly after the smelting process, while the spongy iron and slag mass is hot, traditionally considered to be achieved with a wooden hammer; 2) Primary smithing / reheating (consolidation, purification, shaping and standardisation): a) the bloom is reheated in a hearth and subjected to repeated hammering (wooden hammer) to expel entrapped

slag and consolidate the iron particles. The output is a more compact, semi-refined iron mass—often referred to as a consolidated bloom; b) The semi-refined iron is further worked into intermediate forms or semi-products such as bars, billets, or slabs. The latter phase allows for structural homogenisation and standardisation of iron for trade, storage, or subsequent manufacturing of objects. It requires the use of a metal hammer. Techniques at this stage vary depending on the intended use of the metal and the cultural or regional metallurgical traditions.

Although the production process is technically complex and varies across time and space, the resulting semi-products are often described merely as *blooms* or *bars*, accompanied by basic measurements such as weight and maximum dimensions. This descriptive approach permits only limited comparative analysis. Several morphological traits of a bloom or bar may be considered principal attributes for understanding the technological steps involved in their production—such as surface morphology and internal structure (including visible deformations and slag, iron and porosity content). The characteristics of surface structure (if cleaned of corrosion) can inform about methods of handling and procedures carried out (use of wooden or iron hammer, hammering base type, wedging etc.) (Merta 2019). Macroscopic or microscopic examination of cross-sections can reveal slag, porosity, iron content, and plastic deformation from shaping, and may indicate the refining stages applied to iron semi-products (Bauvais, Fluzin 2009; Berranger, Fluzin 2011; Galili et al. 2015; Saage et al. 2018; Strobl et al. 2010; Török et al. 2017; 2018; 2022; 2024). However, these are destructive methods and serve only as relative comparative tools due to the lower accuracy in measuring partial surfaces and the potential structural variability within a semi-product observed, requiring complementary analytical methods. Bulk density constitutes the most complimentary and integrative non-destructive parameter for characterising iron semi-products, as it captures the combined volumetric contribution of metallic iron, slag inclusions, and porosity within the object as a whole. Since the density of a metallic object reflects its internal structure, it could be used as a proxy for evaluating key factors - degree of refinement (technological procedures) and iron content (metallic yield). Standardised density measurements could facilitate comparative studies across sites and periods, revealing regional or chronological similarities and differences in metallurgical processes and technological choices made. Density measurements incorporated into the morphological analysis of archaeological iron semi-products (Dungworth 2015; Espelund 2013; Merta 2019; Pleiner 2000) or experimental testing (Crew 1991) are present in the published works, though very rare, making the comparative study possible only on a limited level. Metallic yield (in form of a bloom or bar) in archaeometallurgical studies is usually calculated through results of experimental smelting and smithing sessions, as a ratio ore : slag : bloom/bar/billet or through combination of experimental testing and chemical analyses of resources and waste (Crew 1991; Crew, Crew 1994; Dillmann et al. 1997; Eschenlohr, Serneels 1991; Joosten et al. 1998; Karavidović 2020; Senn 2001; Thiele, Török 2011; Tylecote et al. 1971). However, the total iron content (Fe%) of a given iron-semi-product remains a key, unaddressed question. Simple bulk density measurement could enable quantitative estimation of iron content and metallic yield, and improve the understanding of production efficiency and past iron economies. A quantifiable metric (like iron percentage) improves classification schemes for semi-products—beyond just size and shape—by incorporating an element of material quality.

The iron production *chaîne opératoire* reflects not only the technical expertise embedded in early ironworking but also the socio-economic and cultural frameworks in which it was practiced. A standardised analytical protocol for describing and categorising each technological stage is essential for meaningful comparative studies of metallurgical practices across chronological, geographical, and cultural boundaries.

The objective of this research is to propose a framework for a basic morphological descriptive standard to support the identification of refinement levels and the estimation of iron content in archaeological iron semi-products. Such a standard facilitates the reconstruction of the technological processes involved in their production and enables the assessment of usable iron yield from individual semi-products. The proposed approach is informed by a series of experiments replicating key stages associated with the production of iron semi-products, including direct reduction and post-reduction refinement. Based on the results of experimental testing, a classification system grounded in object density is proposed for differentiating between stages of refinement. Furthermore, a physically grounded three-phase theoretical model (iron–slag–porosity) that explains how measured density relates to iron, porosity and slag content during post-reduction processing is established and a predictive correlation between density and iron content is established through linear regression based on the experimental forging of compacted and reheated blooms into purified bars. Finally, an equation for calculating the estimated mass of an iron semi-product in different stages of refinement is introduced.

2. Materials and methods

To achieve the objectives of this research, a programme of experimental testing, theoretical and predictive modelling was devised. The experimental setup and predictive modelling has three principal aims:

1. To define density ranges corresponding to different levels of refinement in iron semi-products;
2. To estimate the iron content (Fe%) within a given semi-product and enable estimation of the mass of an iron semi-product at any given density;
3. To apply and compare these findings to available archaeological finds.

2.1. Experimental testing

To address the initial objective, 35 iron semi-product samples were produced by direct reduction and subsequently refined through post-reduction procedures.

The direct reduction was carried out in a reconstruction of early medieval shaft furnaces, with a shallow hearth and freestanding or/and semi-dug in clay shaft, known as Nemesker and Avar type furnaces after J. Gömöri (2000). These furnaces measure from 28-40 cm in inner diameter of the hearth, reach 60-70 cm in height and have a plate ("door") with incorporated tuyere at the front, that was removed for the extraction of the bloom (Gömöri 2000; Sekelj Ivančan, Karavidović 2021). These types of furnaces were widespread within Carpathian basin and its fringes, namely Transdanubia in Hungary, Burgenland in Austria and Podravina region in Croatia from 7th to 9th centuries and appear in Moravia in the Middle Hillfort period (800-950 AD) (Gomori 2000; Bielenin 1977; Mehofer 2010; Kerbler–Krainz 2013; Sekelj Ivančan–Karavidović 2021; Souchopová 1986: 23–37, fig. 28).

Different types of ores were used in the experiments, including regional bog iron ore found in the lowland areas of the Pannonian basin, todays Hungary and Croatia (Brenko et al. 2020; 2021; Kercsmár, Thiele 2017). Smelting was conducted by intermittently charging 300 g portions of ore and charcoal in a 1:1 ratio. The average air input ranged from 150 to 300 L/min. Charcoal had a grain size of 6–50 mm, while the ore was roasted and crushed to 4–18 mm, with finer particles sieved out. The experimental smelts lasted between 3 and 9 hours, depending on the total amount of ore charged. The aim was to produce blooms ranging in size and weight from 1 to 11 kg (reflecting different stages of refinement), comparable to semi-products known from the Iron Age, Roman and the Medieval period in South-Central Europe and Scandinavia (Gömöri 2000; Espelund 2000; Pleiner 2000; 2003; Merta 2019; Souchopová, Stránský 1999). The experimentally produced blooms, representing various stages of refinement, weigh between 1,3 and 5 kg, with two samples weighing 8,7 kg and 9,2 kg.

The post-reduction techniques applied were intended to reconstruct potential stages in the production of iron semi-products, as evidenced by historical records and supported by morphological and archaeometric analyses of archaeological semi-products (Pleiner 2000; 2003; 2006; Buchwald 2005). The experimental primary smithing was conducted by a single individual. The experimentally produced semi-products can be defined as follows: 1) **Iron sponge**: uncompacted bloom, as extracted directly from the smelting furnace; 2) **Compacted iron bloom**: hot-hammered with a wooden hammer on a wooden log as anvil immediately after extraction; 3) **Consolidated iron bloom**: bloom purified and consolidated by reheating and hammering using a wooden hammer on a wooden log as anvil to a maximum achievable level; 4) **Iron bar**: consolidated bloom reheated and further purified using an iron hammer, on an iron anvil without flux use or welding. Compaction of an iron sponge was executed within several minutes, until cooled. Reheating was carried out in a simple side-blown reheating installation (Figure 1). Reheating time and number of reheats applicable was variable, depending primarily on base-state of the processed sample (structural integrity/compaction level), size of the sample and delivered air input (hot zone size), ranging between 30-45 min and 2-5 heating cycles. The wooden hammer used was 3,5 kg heavy, with an impact surface of 12 cm diameter and velocity was between 5 and 10 m/s.

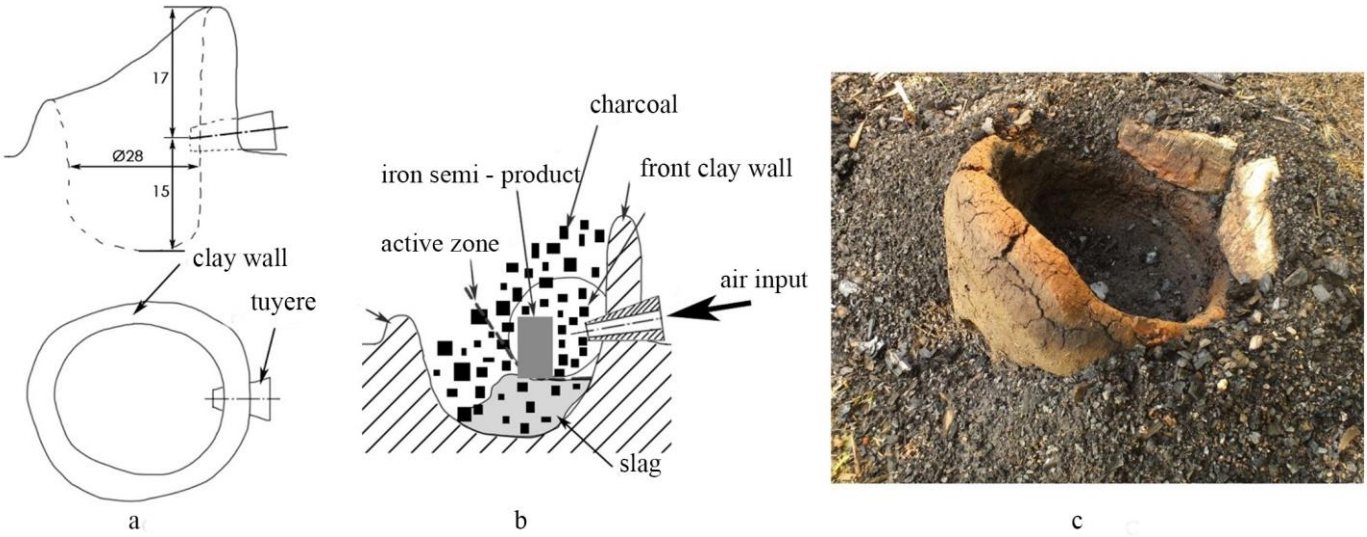

Figure 1 Side-blown forge used in the experiments: a) graphical representation of geometry of the forge, b) graphical representation of the reheating process, c) forge after the reheating, cleaned of slag residue and unburned charcoal.
1. Ábra: A kísérleteknél használt oldalszeles kovácstűzhely: a) a kovácstűzhely oldal és felülnézeti képe a főbb méretekkel, b) a kovácstűzhely főbb részei, c) fotó a kovácstűzhelyről

To address the second objective—determining the iron content of semi-products based on their density—five experimental bloom samples at various stages of refinement (compacted and reheated), together with one archaeological sample from the Iron Age site of Jakab-hegy (Hungary), were forged into bars. The blooms were heated in a simple, conventional side-blown forge (Figure 1).
Charcoal with particle sizes of 12–25 mm and 25–50 mm was used, and the air blast ranged from approximately 200 to 500 l/min. The iron bars were forged through 4–5 heating cycles over a period of 30–45 minutes using a mechanical Ajax2 power hammer, weighing 60 kg, with an impact surface of 18x5 cm at velocity between 0,5 and 1 m/s. Burn-off losses during the experiments were minimal due to the rapid and limited heating, so only a negligible amount of the iron phase was lost as hammerscale. In order to avoid more significant iron losses and to more closely replicate archaeological iron bars known to retain slag inclusions, the bars were not forged to full purification (i.e., to a nearly slag- and crack-free state). Instead, forging was limited to achieving a density exceeding ca. 7, 0g/cm³ without further reheating.
Density of each semi-product was calculated using Archimedes water displacement measurement (Figure 2).

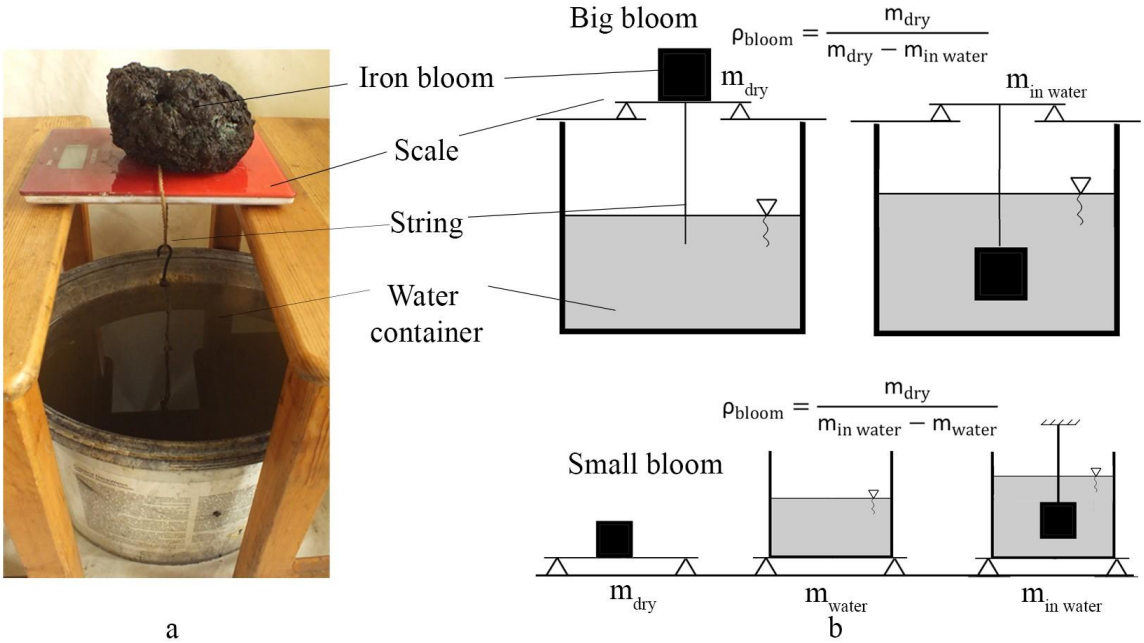

Figure 2 Density measurement using the water displacement principle: a) measurement setup, b) graphical representation for measurement of bigger (top) and smaller (bottom) blooms.
2. Ábra: Sűrűségmérés vízkiszorításos elven. a) fotó a mérési elrendezésről, b) a sűrűségmérések vázlatos bemutatása nagy- (felül) és kisméretű (alul) vasbucára.

2.2. Theoretical and experimental predictive modelling

To propose a theoretical material model, four semi-products, representing different stages of refinement were cross-cut, and the structure is analysed visually to determine the constituent phases and relative relation between content. Visual observations are complemented by quantitative cross-section image analysis to quantify phase proportions in these iron semi-products. False-colour overlays of objects cross-section images were generated in Adobe Photoshop using a Magic Wand Tool (Tolerance=20). This ensured consistency between quantitative results and spatial distribution patterns visible on the samples. Surface colour proportions were quantified using a pixel-based image analysis approach. Transparent pixels and near-white background pixels were removed using RGB thresholding, ensuring that only the object surface was included in subsequent calculations. Based on luminance, pixels were classified into three tonal categories: Black: luminance < 50; Dark grey: luminance 50–139; Light grey: luminance ≥ 140. For each category, pixel counts were calculated and expressed as percentages of the total object surface area.

Based on this, a model for calculation of slag, porosity and iron content is proposed. The six blooms experimentally forged to bars are further taken as case study example for determining a predictive model calculation of iron content (Fe%) as a function of density (ρ) via linear regression. The iron, porosity, and slag contents predicted by the model are compared with independent cross-section image surface analyses of experimental blooms. Finally, the equation for prediction of mass of any given semi-product in different stages of refining is derived based on estimated iron content and density of the semi-product.

2.3. Archaeological samples

To evaluate the complementarity of the density values and ranges obtained from experimental samples with the archaeological samples, iron semi-products from archaeological contexts dated to the Iron Age and Early Medieval period were analysed, along with data from a literature review. As data on bulk density is rarely measured and reported, the literature review gave only limited results. The selection of the samples is based primarily on methodological grounds following experimental replication presented here. This relates to size and weight of the experimental blooms, as well as potentially comparative smelting furnace capacity and type. All samples come from sites within the of Carpathian basin, and areas in immediate vicinity. Samples dated to Early Middle Ages, are from in Transdanubia (Hungary) and Moravia (Check Republic). They represent typically sized blooms of the early Middle Ages, both smaller weight category (1-5 kg) and larger one (8,5-10 kg), which is related to smelting furnace type and/or capacity used in experimental reconstruction.
Iron Age samples from the Jakab-hegy site are contextually connected to the bloom experimentally forged into a bar, obeying the methodological premise of size and weight, and comprise blooms recovered from a single context: a deposit consisting exclusively of iron blooms found within a shallow pit at the Jakab-hegy site near Pécs. The site has occupation phases dating to the Early Iron Age (Ha C/D) and the Late Iron Age (LT C/D). As no associated finds allowing a more precise chronology were present, the deposit can only be broadly dated to Iron Age i.e. the phases defined on site. Another sample, found as a surface find within spatial extent of a site dated into the Early Iron Age, from Verebce-bérc is analyzed as it falls well within size/mass range experimentally tested, and the results of analysis can be compared to published metallographic analyses of the archaeological semi-products from the same site.

3. Results

3.1. Density ranges and stage-based classification of semi-products

Density measurements of experimental iron semi-products (Table 1, Figure 3) allow classification into four main categories, each corresponding to a specific post-reduction refinement stage as defined previously:
(1) ρ = 3–4 g/cm³ – uncompacted iron sponge;
(2) ρ = 3,5–5 g/cm³ – compacted iron bloom;
(3) ρ = 5–6 g/cm³ – reheated/consolidated iron bloom;
(4) ρ ≈ 7,3–7,7 g/cm³ – iron bar
The density of an object increases in correlation with the degree of purification achieved during the refining process, ultimately approaching—but remaining slightly below—the density of pure iron (7,87 g/cm³) in the case of iron bars. If observed among archaeological material, densities of 6 – ≈ 7,3 g/cm^3 could be regarded as heavily refined iron blooms or loosely consolidated bars (iron hammer and anvil), depending on other morphological factors. These densities were not recorded among experimental samples since the last stage of refining aimed at replicating heavily purified iron bars, and refining with wooden hammer showed limited to

gaining a density of 6 g/cm^3. The calculated impact (m*v/A) for the wooden hammer used in refining the blooms up to the consolidated state (5-6g/cm^3) was approximately 1,5–3,1×10^3 kg/m*s. The threshold of 6g/cm^3 is defined as the maximum achievable density with given parameters. The iron hammer used has a calculated impact of 3,3–6,7 ×10^3 kg/m*s. The clear separation between these ranges reflects fundamentally different mechanical regimes: wooden hammering is sufficient primarily for collapse of large, interconnected pore networks and limited slag redistribution, whereas iron hammering delivers stresses high enough to expel finer slag inclusions and close residual micro-porosity. The calculated impact contrast therefore provides a physically grounded explanation for the experimentally observed density threshold of ~6 g/cm³ attainable with wooden tools and the substantially higher densities achieved during bar formation using iron hammer and anvil.

The results indicate that an object's technological treatment can be inferred from its density, measured simply and non-destructively using the Archimedes' method.

Table 1 Experimental samples of iron semi products with variable degree of postreduction processing (see Figure 3).
1. Táblázat: Kísérleti próbakohósítások során előállított vasbucák sűrűsége különböző tömörítettségi állapotban

Sample	Semi-product	Tool	Process	Weight (kg)	Density (g/cm^3)	Density range (g/cm^3)
1	iron sponge	/	uncompacted	5,20	3,20	3,2 - 4,05
2				0,75	4,05	
3	iron bloom	wooden hammer / wooden log anvil	compacted	2,60	3,60	3,5-5,0
4				2,40	3,60	
5				2,37	3,63	
6				4,40	4,00	
7				3,60	4,00	
8				2,00	4,50	
9				4,10	4,50	
10				3,54	4,52	
11				1,70	4,66	
12				1,30	4,70	
13				1,26	4,84	
14*			reheated	8,70	4,90	5,0-6,0
15				1,27	5,00	
16*				9,20	5,10	
17				2,48	5,13	
18				1,28	5,14	
19				0,84	5,14	
20				2,48	5,15	
21				3,21	5,16	
22				1,84	5,28	
23*				4,90	5,30	
24				1,27	5,37	
25				1,60	5,78	
26				1,60	5,89	
27*				2,40	5,90	
28	iron bar	iron hammer / iron anvil	reheated	2,89	7,19	7,2-7,7
29				1,13	7,22	
30				1,46	7,25	
31				0,93	7,34	
32				1,70	7,40	
33				2,08	7,41	
34				1,50	7,50	
35				1,70	7,68	

*objects wedged

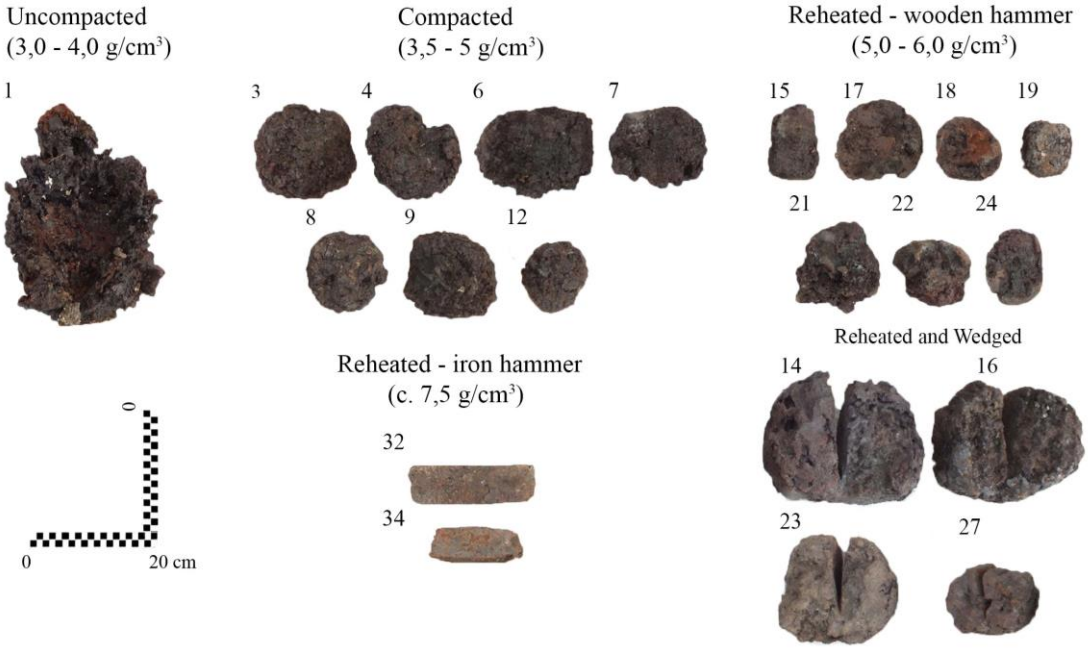

Figure 3 Samples of experimentally produced iron semi-products of different mass, density and level of purification (numbers denote samples in Table 1)
3. Ábra: Kísérleti próbakohósítások során előállított vasbucák fotói (a minták számozása az 1. táblázat adataival összhangban)

3.2. Iron content and mass of iron semi-products through the purification process

3.2.1 Cross-section phase proportions across refinement stages

As a starting point for the modelling, full cross-sections of the experimental samples with varying densities were examined through visual inspection (Figure 4a, c) and quantitative surface analysis (Figure 5) in order to assess their internal structure. The analysis shows highly heterogenous structure across the surface of uncompacted sponge and compacted and reheated blooms (Figure 4c, 5). The cross-sections show that, in addition to the iron and slag phases comprising the bloom, both phases contain porosities. As the degree of purification and material density increase, the proportion of iron rises, while the relative amounts of slag and porosity decrease. This process ultimately results in iron bars characterised by only minor slag inclusions and very limited micro-porosity.

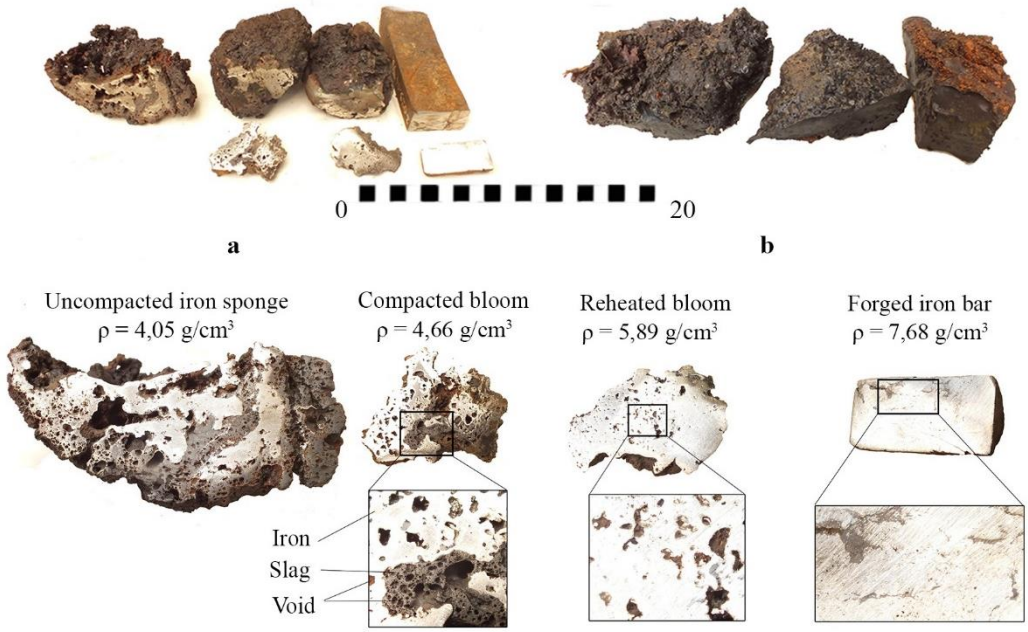

Figure 4 a) Samples cut from iron semi-products of different purification level and density, b) tap slag samples measured for density, c) cross-cut surface of iron semi-products with different purification level and density- uncompacted iron sponge (Table 1: 2), compacted iron bloom (Table 1: 11), reheated iron bloom (Table 1: 26), iron bar (Table 1: 35) (see also Figure 5).
4. Ábra: a) Különböző sűrűségű és tömörítettségű vasbucákból és bucavas tömbből kivágott minták, b) Sűrűségmérésbe bevont folyósalakminták, c) A különböző tömörítettségű vasbucákból kivágott minták csiszolata, tömörítettlen vasbuca (1. Táblázat, 2. minta), tömörített vasbuca (1. Táblázat, 11. minta), újraizzított vasbuca (1. Táblázat, 26. minta), vastömb (1. Táblázat, 35. minta), (ld. még a keresztmetszetek sematikus rajzát az 5. ábrán).

Quantitative analysis of sampled material surfaces in three-phase cross-section images (Figure 5) indicates that metal content increases systematically with density, from an uncompacted iron sponge (59,12 % at ρ = 4,05 g/ cm³) to a compacted bloom (73,48 % at ρ = 4,66 g/cm³), a reheated and consolidated bloom (84,06 % at ρ = 5,89 g/cm³), and finally the iron bar (98.76 % at ρ = 7,68 g/cm³). Over the same density range, porosity declines rapidly at lower density increments, from 19,40 % to 10,54 % and 6,11 %, before falling to 0,14 %, whereas slag content decreases more gradually, from 21,48 % to 15,98 %, 9,82 %, and finally 1,09 %. The transition between intermediate density stages (between 5 and 6 g/cm³) and heavy refining (c. 7,68 g/cm³) marks a shift from predominantly compaction-driven change (porosity closure) to more effective metallurgical refinement, in which slag removal becomes the dominant factor controlling material composition. Porosity exhibits a steep early decline because void closure responds directly to initial compaction, whereas slag decreases more gradually, reflecting progressive removal during repeated thermal and mechanical refinement.

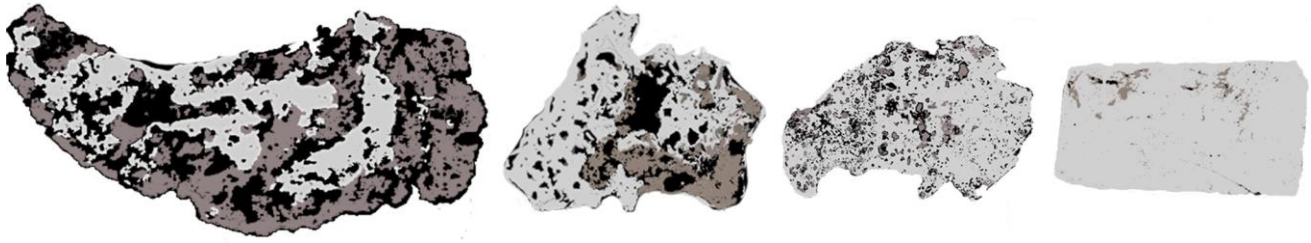

Material category	Sample A	Sample B	Sample C	Sample D
	ρ = 4,05 g/cm³	ρ = 4,66 g/ cm³	ρ = 5,89g/cm³	ρ = 7,68 g/cm³
Metal (light grey)(%)	59,12	73,48	84,06	98,76
Slag (dark grey)(%)	21,48	15,98	9,82	1,09
Porosity (black)(%)	19,4	10,54	6,11	0,14
Total analysed surface area (%)	100	100	100	100

Figure 5 Three-phase surface classifications (original photographs: Figure 4c) and quantitative surface analysis of iron semi-products with increasing density, from an uncompacted iron sponge (Sample A), through a compacted iron bloom (Sample B) and a reheated and consolidated bloom (Sample C), to a fully refined iron bar (Sample D).
5. Ábra: A különböző tömörítettségű vasbucákból kivágott minták csiszolatának semítikus rajza képelemzéshez, tömörítettlen vasbuca (A minta), tömörített vasbuca (B minta), újraizzított vasbuca (C minta), vastömb (D minta).

3.2.2. Theoretical material model

Based on the visual observations (Figure 4, 5**)**, a three-phase material model is proposed in which the iron matrix contains slag inclusions and porosities. As boundary conditions, the density of iron phase is taken as 7,87 g/cm³, while the density of air (porosity) is considered negligible (approximately 0 g/cm³). The density of the slag phase is taken as approximately 3,5 g/cm³, based on density measurements conducted on compact, low viscosity and porosity tap slag samples (Figure 4b). The iron burn-off loss is set to zero, as another boundary condition. Using standard relationships between mass ($m = m_{iron} + m_{slag}$), volume ($V = V_{iron}+V_{slag}+V_{voids}$), and density ($\rho = m/V$), porosity is defined as a volume fraction ($P = V_{voids}/V$), and iron content as a mass fraction ($Fe = m_{iron}/m$). From these definitions, the iron content of the three-phase material can be expressed as a function of density and porosity:

$$Fe = \frac{\rho_{iron} - \rho_{iron}\rho_{slag}\frac{1-P}{\rho}}{\rho_{iron} - \rho_{slag}} = 1{,}8 - 6{,}3\frac{1-P}{\rho} \quad (1)$$

From equation (1) porosity can be expressed as:

$$P = 1 - \rho\left(\frac{Fe}{\rho_{iron}} + \frac{1-Fe}{\rho_{slag}}\right) = \frac{Fe-1{,}8}{6{,}3}\rho + 1 \quad (2)$$

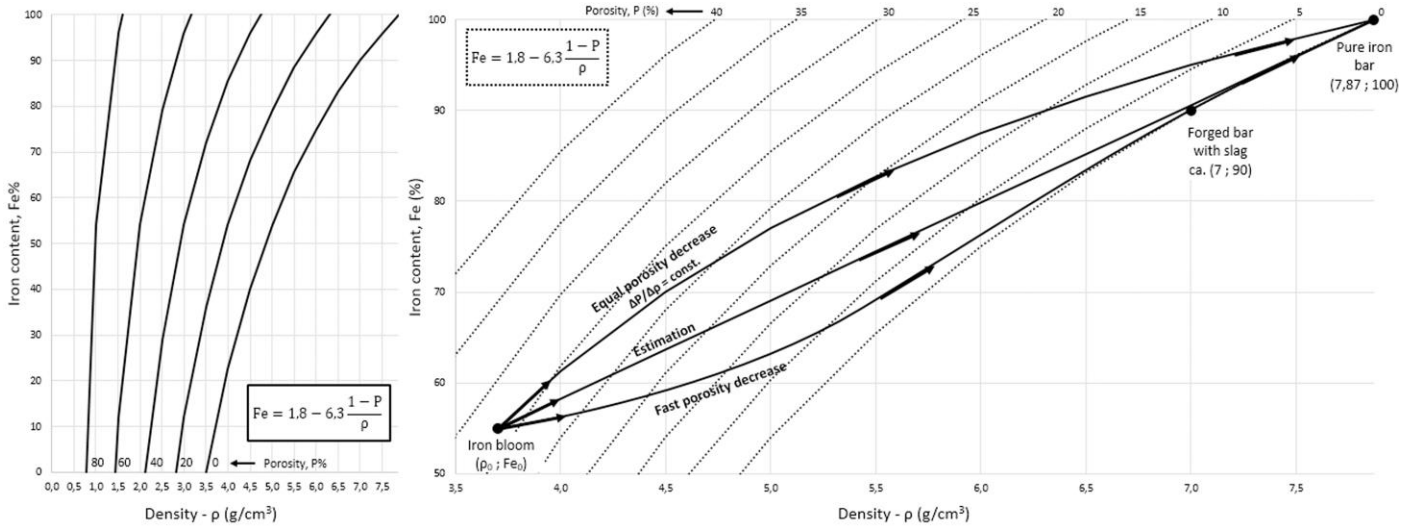

Figure 6 a) The theoretical iron content (Fe) as a function of density (ρ) and different porosity content (P), b) Theoretical iron content graphs through the postreduction refining from uncompacted iron sponge to an iron bar.
6. Ábra: a) Az elméleti vastartalom (Fe) a sűrűség (ρ) és a porozitás (P) függvényében a három fázisú anyagmodell alapján. b) Az elméleti vastartalom lehetséges változásai egy vasbuca vastömbbé kovácsolása során.

Figure 6a illustrates the theoretical iron content (Fe%) as a function of density (ρ) for a set of fixed porosity values (P%), calculated using equation (1). Each curve represents a static material state with constant porosity, illustrating the combined influence of density and porosity content on the iron fraction. Figure 6b extends this framework to refining processes by illustrating possible evolutionary trajectories during the forging from an uncompacted iron sponge into a bar. In this diagram, the dotted curves correspond to porosity states as shown in Fig. 6a, while the solid arrows represent dynamic forging paths in which both porosity and density change. If a simplified forging behaviour is assumed, in which porosity decreases proportionally with increasing density ($\Delta P/\Delta\rho$ = constant) through the process of reheating and forging, porosity can be expressed as a linear function of density and substituted into equation (1). This substitution results in a non-linear (hyperbolic) relationship between iron content and density, expressed by equation:

$$\mathrm{Fe} = 1{,}8 - 6{,}3\frac{(1-\mathrm{P})}{\rho} = 1{,}8 - 6{,}3\frac{\left(1-\frac{\Delta\mathrm{P}}{\Delta\rho}(\rho_{\mathrm{iron}}-\rho)\right)}{\rho} = 1{,}8 - \frac{6{,}3}{\rho} + \frac{\Delta\mathrm{P}}{\Delta\rho}\left(\frac{50}{\rho} - 6{,}3\right) \qquad (3)$$

The corresponding trajectory is shown by the upper solid curve in Fig. 5b. While this model is mathematically consistent, it implies that porosity reduction and slag removal proceed at comparable rates throughout the forging process, i.e. porosity decreases equally through the process. However, based on experimental observations and comparative quantitative analysis of cross-section surfaces (Figure 5), a more realistic behaviour should assume a fast porosity decrease in the beginning of the forging, declining through the process. At densities of approximately 7 g/cm³, porosity can be assumed to approach zero, and further increases in density primarily reflect slag expulsion. This path is represented by the lower curve in Fig. 6b. The slag content however, is removed significantly slower than porosity and gradual decrease of slag content should be expected through the process. Under these conditions, the relationship between iron content and density can be reasonably approximated as linear over the main forging interval (middle trajectory on Figure 6b). This approximation does not imply linearity over the entire forging sequence, but provides a practical estimate of iron enrichment during the dominant phase of bar formation.

3.2.3. Experimental calibration: The estimated iron content (Fe%) (regression model)

The second experimental set resulted in successful forging of five experimentally produced blooms and one archaeological sample into bars (Figure 7). On the basis of these experiments and the theoretical iron content model, the percentage of iron within a given semi-product as a function of density can be estimated.

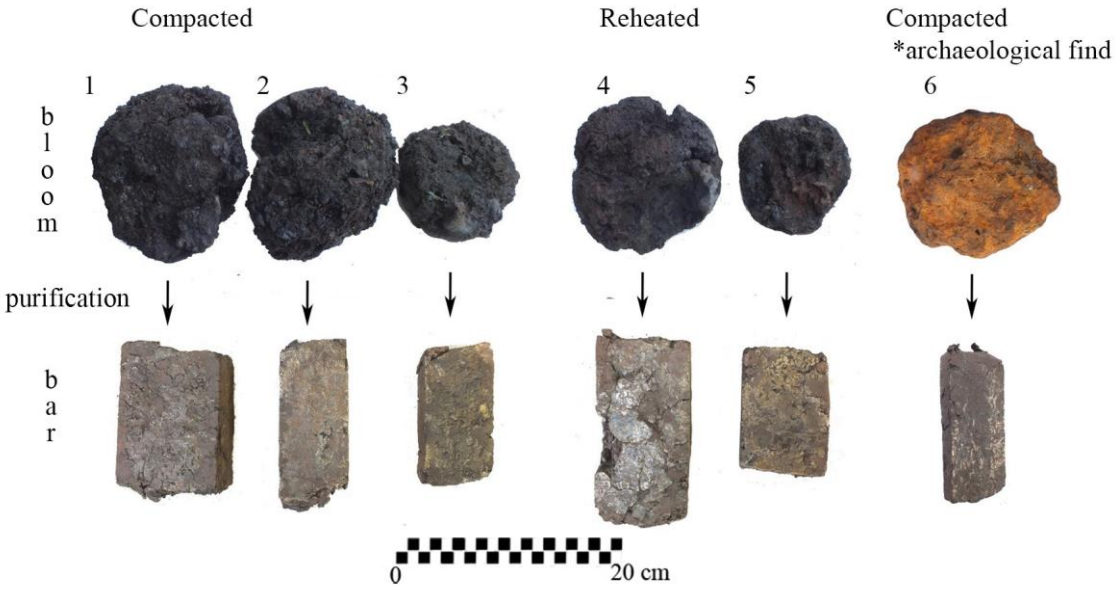

Figure 7 Experimental samples – compacted (1-3, 6*) and reheated (4-5) iron blooms forged into iron bars (1-5', 6*') (Table 2)
7. Ábra: A kovácsolási kísérletekbe bevont vasbucák (1-3, 6* – tömörített és 4-5 – újraizzított vasbucák) és a belőlük kikovácsolt vastömbök (1-5', 6*') (ld. még 2. táblázat).

The iron content of the bars (Fe'%) can be derived using equation (1), with measured mass (m') and density (ρ') of the bars. The porosity of a forged bar is assumed to be negligible as a boundary condition (cf. Fig. 4), and set to zero. The mass of the metallic iron ($m_{metallic\ iron}$) can therefore be calculated as $m_{metallic\ iron} = m' \cdot Fe'\%$. Assuming negligible burn-off losses during forging as further boundary condition, the metallic iron content of the initial semi-product (i.e. the compacted or reheated bloom) is considered equal to that in the final iron bar. The iron content of the initial semi-product can thus be calculated as $Fe_0\% = m_{metallic\ iron} / m_0$. On this basis, the porosity (P_0%) of the initial semi-product can be calculated from equation (2). The measured and calculated data for iron blooms nr. 1-6* and bars 1'-6*' are summarized in Table 2.

Table 2 Measured, calculated and estimated values of mass (m), density (ρ), iron content (Fe%) and porosity (P%) of experimental iron semi-products (including archaeological sample 6*), in their initial state and after purification/forging into bars.
2. Táblázat: A mért, számított és becsült tömeg (m), sűrűség (ρ), vastartalom (Fe%) és porozitás (P%) értékek a kovácsolási kísérletekbe bevont vasbucák és a belőlük kovácsolt vastömbök esetén.

Bloom						Bar					Bloom		
Sample	Initial stage	Measured		Calculated (theoretical model)		Sample	Measured		Calculated (theoretical model)			Estimated (regression model)		
		m_0 (g)	ρ_0 (g/cm^3)	Fe_0 (%)	P_0 (%)		m' (g)	ρ' (g/cm^3)	Fe' (%)	$m_{metallic\ iron}$ (g)	P' (%)	Fe (%)	$m_{metallic\ iron}$ (g)	P (%)
1	compacted	3538	4,52	75,5	25,0	1'	2890	7,19	92,4	2671	0	68,6	2427	20,0
2	compacted	2365	3,63	57,4	29,4	2'	1458	7,25	93,2	1358		60,4	1428	31,1
3	compacted	1262	4,84	69,6	15,1	3'	932	7,34	94,2	878		71,5	903	16,6
4	reheated	2478	5,15	79,6	17,9	4'	2076	7,41	95,0	1973		74,4	1843	13,6
5	reheated	1273	5,37	82,1	16,6	5'	1127	7,22	92,8	1046		76,4	973	11,7
6*	compacted	1988	4,37	60,5	17,1	6*'	1231	7,65	97,7	1203		67,2	1336	21,7

The results indicate that the iron content of compacted blooms is lower than that of reheated and refined blooms, and, naturally, lower than that of the final iron bar. The highest porosity, approx. 30%, is presumed in sample 2, a very lightly compacted bloom which has the lowest density. The variability between calculated iron content of the samples, especially illustrated by differences in calculated iron contents of samples 1 and 6* (Table 3), that have a similar density (4,52 g/cm^3 vs. 4,37 g/cm^3) is inherent due to the nature of the calculation, and differences in the initial mass of the samples (3538 g vs. 1988 g).

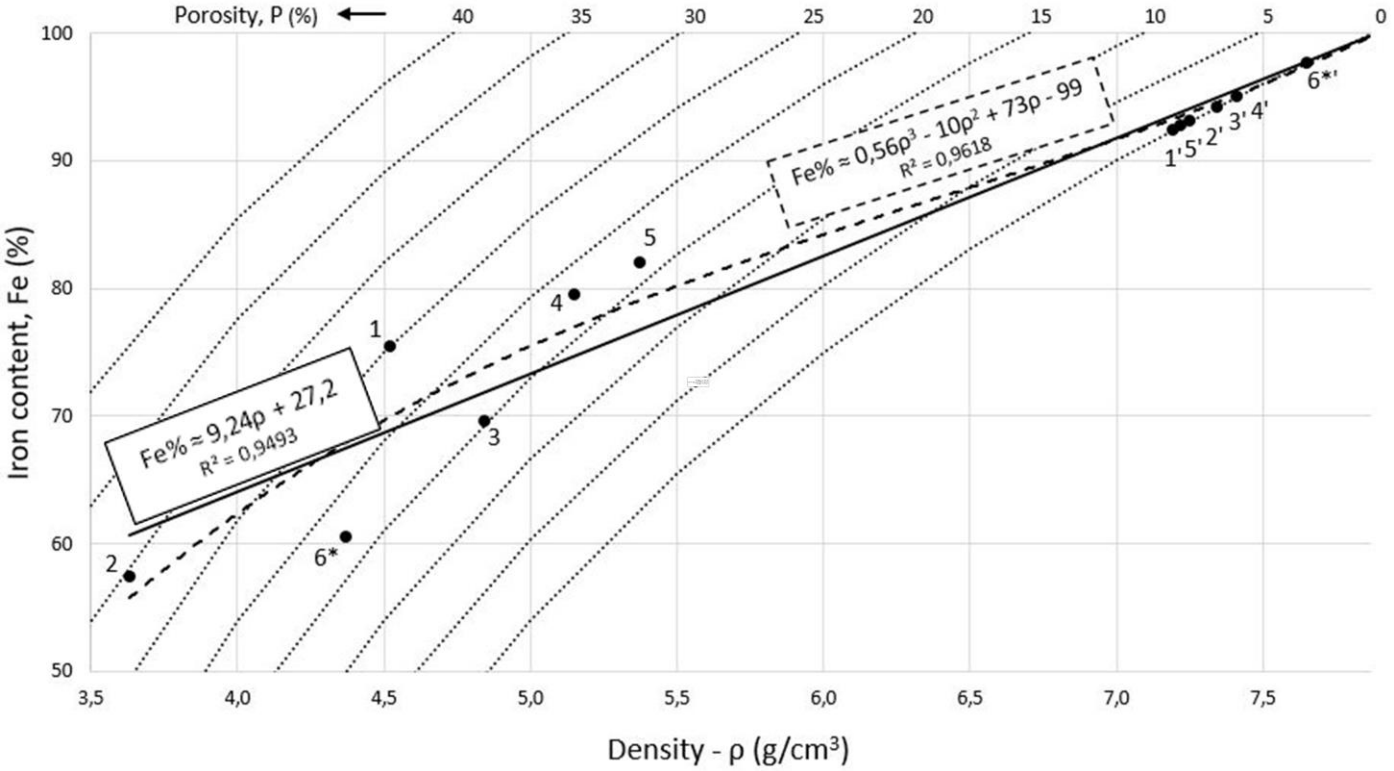

Figure 8 The estimated iron content – calculated iron content (Fe%) of the experimental samples (Table 2) as a function of measured density (ρ), with the and porosity contours and the fitted regression model for estimating the iron content.
8. Ábra: A becsült vastartalom – a kovácsolási kísérletekbe bevont vasbucákra és a kikovácsolt vastömbökre számított vastartalom értékeknek megfelelő pontok a sűrűségek függvényében és az ezekre illesztett, a sűrűség függvényében a becsült vastartalmat mutató regressziós egyenes

Building on the theoretical material model, in order to establish a general relationship between density and iron content in iron semi-products weighing several kilograms, a linear regression model was applied on experimental data (Figure 8). The resulting equation for the estimated iron content is as follows:

$$Fe\% \approx 9{,}24\rho + 27{,}2 \qquad (4)$$

The correlation coefficient between the samples indicates a strong positive relationship (r = 0,98), and the coefficient of determination for the regression model is high (R^2 = 0,95), suggesting that the model provides a reliable approximation and accounts for a substantial proportion of the variance. In comparison, the coefficient of determination for a cubic polynomial regression is somewhat higher ($R^2 \approx 0{,}96$), and could be used as well. However, the linear regression model is preferred due to its simplicity that refers on the estimation as well as the rounded constants in Equation (4), which would be Fe% ≈ 9,2346ρ + 27,193 in a more accurate form. Using Equation (4), the iron content (Fe%), porosity (P%), and mass of metallic iron ($m_{metallic\ iron}$) are estimated for all experimental samples and summarised in Table 2.
When equation (4) is applied to experimentally established density categories, the estimated iron and porosity contents are:
(1) ρ = 3–4 g/cm³ – uncompacted iron sponge, Fe ≈ 55-64 %, P ≈ 40-26%;
(2) ρ = 3,5–5 g/cm³ – compacted iron bloom, Fe ≈ 60-73 %, P ≈ 33-15%;
(3) ρ = 5–6 g/cm³ – reheated/consolidated iron bloom, Fe ≈ 73-82 %, P ≈ 15-7%;
(4) ρ ≈ 7,3–7,7 g/cm³ – iron bar, Fe ≈ 94-96 %, P ≈ 0,5 – 0%.
Ultimately, the density of pure iron is 7,87 g/cm³—which is not realistic for archaeological bar finds—would correspond to 100% iron content. With the presented form of formula (4) the iron content equates to 99,998 % of iron. The formula is applicable to densities of iron semi-products of ρ >3 g/cm^3.
The quantitative cross-section surface data shown in Figure 5 correspond closely with estimated density-based compositional ranges for successive stages of iron consolidation and refinement. At low densities (Sample A , ρ ≈ 4,05 g/cm³), the uncompacted iron sponge falls within the reference range for metal and porosity, albeit towards its more consolidated end. The compacted bloom (Sample B, ρ = 4,66 g/cm³) matches the upper limits of the reference range for compacted material, while the reheated and consolidated bloom (Sample C, ρ = 5,89 g/cm³) slightly exceeds the upper iron content and approaches the lower porosity bound of the corresponding

range. The final iron bar (Sample D, ρ = 7,68 g/cm³) shows excellent agreement with reference values for refined bars. Overall, the measured data closely align with established density–composition. The slight differences can be understood as inherent to heterogeneity of the internal structure of the bloom, since only a single surface per purification stage and individual sample is analysed.

3.2.4. Mass of the iron semi-product through purification process

If the mass (m_0) and density (ρ_0) of an iron semi-product are known (measured), its mass at any stage of post-reduction processing (m_{sp}) —corresponding to a different density—can be estimated from the iron content equation (4) by:

$$m_{sp} = m_0 \frac{9{,}24\rho_0 + 27{,}2}{9{,}24\rho + 27{,}2} \quad (5)$$

The calculated mass of an iron bar (ca. ρ ≈ 7,3–7,7), when applied to archaeological bloom objects, may be interpreted as representing the forgeable iron mass of the bloom, corresponding to purified iron bar that retains some slag inclusions and micro porosities, intendent for further, secondary smithing into objects.
When plotted with the experimental data (Figure 9), where m_0 corresponds to initial bloom mass (Table 2:1-6), the non-linear relationship between density increases and mass loss during post-reduction processing is evident. The curves, derived from Equation (5), show that the majority of material loss occurs at lower densities corresponding to processing of uncompacted iron sponge, gradually declining through the process, while mass stabilises as density approaches that of forged iron bar. The latter is in line with general experimental observations and the theoretical model. Experimental data dots that represent measured values of final iron bars (Figure 9: 1-6'), closely follow the estimated trajectory, albeit both minor under- and over-estimation of final semi-product mass is present.

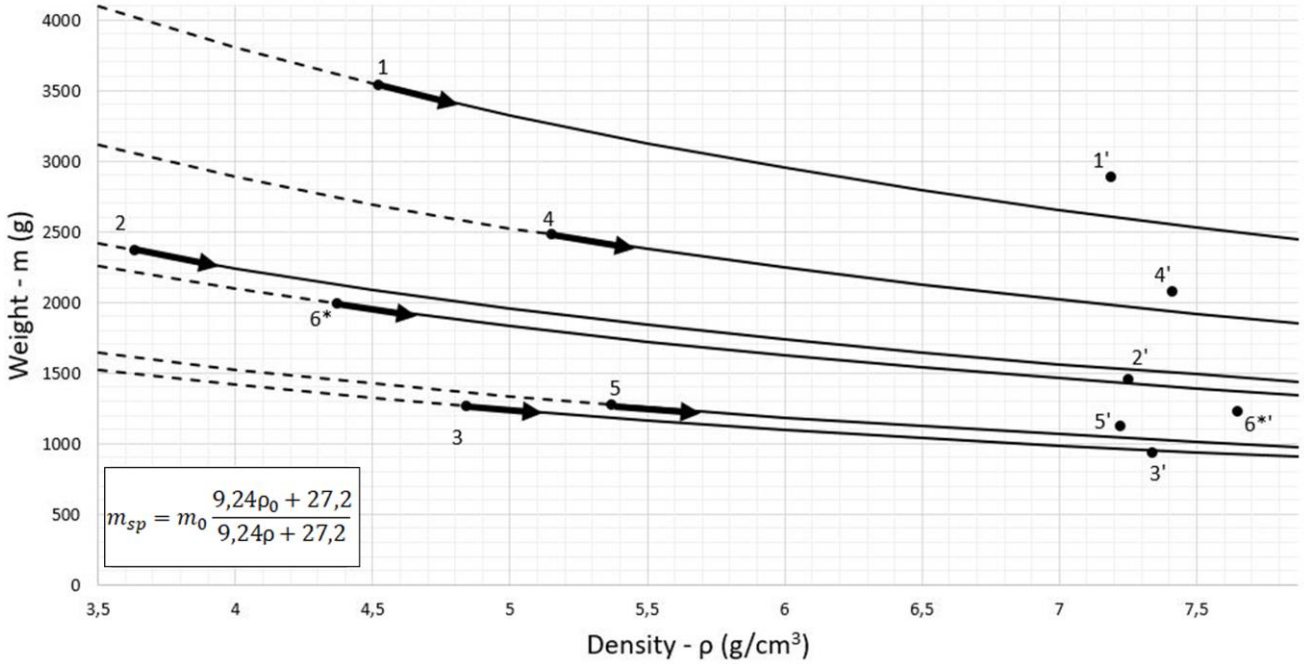

Figure 9 The estimated mass of the iron semi-product – for a full density range experimentally observed: from uncompacted iron sponge (ρ ≈ 3,5 g/cm³) to pure iron bar (ρ = 7,87 g/cm³). Dots (1-6) represent the measured values of experimental samples
9. Ábra: A becsült tömeg – a vasbuca becsült tömege a vastömbbé kovácsolás során a teljes sűrűségtartományra kiterjesztve: a tömörítettlen vasszivacstól (ρ ≈ 3,5g/cm³) a tiszta vastömbig (ρ = 7,87 g/cm³). A diagramban feltüntettet pontok a kísérletbe bevont vasbucák és a belőlük kovácsolt vastömbök sűrűség – tömeg adatpárjait jelölik.

Variability in mass loss relative to density increase is evident among the experimental cases. To enable direct comparison between samples, measured values are normalised to a common final bar density (ρ_2= 7,5 g/cm³), corresponding to a metallic iron content of approximately 96% (Fe_2), calculated by equation (1)(Table 3). This normalisation is achieved by recalculating the final bar mass (m_2) for each bloom from its calculated metallic iron content (Eq. 1). Given that all experiments were conducted under a maximal degree of similarity in processing parameters—including reheating conditions, tools, and smithing technique—the observed mass

loss is directly comparable across samples and cannot be attributed to differences in handling. Instead, it reflects a combination of slag expulsion and metallic iron burn-off during post-reduction processing, with any variation primarily related to intrinsic properties of the individual blooms. Relative mass loss was calculated as $\Delta m = m_0 - m_2/m_0$ and expressed as a percentage. Finally, the mass loss per unit of density increase is expressed for each case (Table 3).

Table 3 Calculated mass change (Δm) and density increase (Δρ) and their ratio, normalised to a final density of ρ = 7,5 g/cm³.
3. Táblázat: A kovácsolási kísérletekbe bevont vasbucák számított tömegcsökkenése (Δm) és sűrűségnövekedése (Δρ) a kapott vastömbök sűrűségét egységesen ρ = 7,5 g/cm³-re átszámítva.

Bloom							Bar					
Sample	Initial stage	m_0 (g)	ρ_0 (g/cm³)	Fe_0 (%)	P_0 (%)	$m_{metallic\ iron}$ (g)	ρ_2 (g/cm³)	Fe_2 (%)	m_2 (g)	Mass loss Δm (%)	Density increase Δρ (g/cm³)	Mass loss / Density increase Δm/Δρ (%/g/cm³)
1	compacted	3538	4,52	75,5	25,0	2671	7,5	96	2782	21,4	2,98	7,2
2	compacted	2365	3,63	57,4	29,4	1358			1414	40,2	3,87	10,4
3	compacted	1262	4,84	69,6	15,1	878			915	27,5	2,66	10,3
4	reheated	2478	5,15	79,6	17,9	1972			2055	17,1	2,35	7,3
5	reheated	1273	5,37	82,1	16,6	1045			1089	14,5	2,13	6,8
6*	compacted	1988	4,37	60,5	17,1	1203			1253	37,0	3,13	11,8

The lowest mass loss values are observed in reheated blooms (approximately 14–17%), whereas the higher values occur in compacted-only blooms with low initial density (21-40%) reaching the highest value with bloom with lowest density (Table 3). This pattern illustrates the trajectory in which mass loss is strongly dependent on initial density. Structurally more refined blooms require less intensive processing (less reheating), and consequently their mass loss is lower. However, burn-off loss of metallic iron—is also influenced by the mass and size of the bloom. Larger blooms with greater initial weight may exhibit proportionally lower metallic iron losses owing to a smaller specific surface area exposed during forging. This effect is evident when comparing Samples 1 and 6*, which have similar initial densities ($\rho_0 \approx 4{,}4–4{,}6$ g/cm³) but markedly different initial masses. Sample 1 shows a mass loss of approximately 21%, whereas the archaeological sample (Sample 6*) exhibits a higher value of nearly 37% (Table 3) i.e. the ratio of mass loss and density increase varies beetween 7,2 and 11,8.

3.3. Archaeological semi-products: density range comparison and case study application

The density values recorded for the analysed archaeological blooms and literature review, ranging from 3,3 to 5,95 g/cm³ (Table 4, Figure 10) correspond closely to those observed in experimental samples (Table 1 and 2). The relatively limited variability observed suggests predominantly no or low to moderate levels of post-reduction refinement, extending from uncompacted iron sponges to compacted blooms. Only two samples exhibit evidence for more advanced purification through reheating, attaining densities approaching 6 g/cm³, which experimental results indicate as the upper limit achievable through reheating and hammering with a wooden hammer (Table 4: Samples 2 and 18). The density ranges—3,3–5,7 g/cm³ for Early Medieval samples and 3,4–5,9 g/cm³ for Iron Age specimens—do not suggest temporally conditioned variation in density range obtained through the postreduction processes. They are consistent with the observations of R. Pleiner (2008), who noted that the majority of blooms fall within a density interval of approximately 3,5–6 g/cm³. Taken together, it could be reasonably inferred that the observed archaeological densities also implicate the boundary condition of density that was reached by compacting with a wooden hammer, especially for blooms weighing between 1-6 kg, as experimental samples.

Since data on the iron blooms presented here is only of limited contextual and chronological comparability, only multiple finds from single context can be analysed in more detail.

Similarities or differences in the level of refinement and iron content are evident among samples from the same archaeological site and period. The Iron Age samples from the Jakab-hegy site (Table 4: 13-17) were found together in a shallow pit depot, recognised on the surface on the multi-phase Iron Age site Jakab-hegy. The samples show some variability in weight and density, however, all within range from uncompacted sponge to compacted blooms density values, implicating a unique, albeit slightly variable, post-reduction processing within the group. The shape of the blooms is not fully standardised (Figure 10), which compliments the limited variability in processing premise. Minor differences in overall mass and estimated metallic iron content are also present, suggesting another variable, the difference in smelting outcomes. Nevertheless, the samples can

be regarded as quite standardised semi-products, as only very limited differences are present, all within the same boundary conditions of lower stage of post-reduction processing and tools used. An interesting point is the difference between the Iron Age samples from Jakab-Hegy (compacted) and Verebce-bérc (reheated). Comprehensive comparative analysis of these differences in not possible due to available limited sample quantity and archaeological contextual and temporal determination of the samples (Table 4), however, it can be stated that the differences in processing are substantial. The sample from Verebce-bérc (Table 4: Sample 18) was recovered as a surface find in 2007 within a hoard of similar semi-products (Török et al. 2011). Although the find context does not allow precise chronological attribution, the sample originates from within the spatial extent of the site Dédestapolcsány-Verebce-bérc, where subsequent archaeological investigations identified a large number of iron semi-products and objects deposits (approximately 30), attributed to the Early Iron Age in the Carpathian Basin (Szabó et al. 2022). Several samples from one deposit, containing total of 96 iron semi-products, dated to end of the 7th century – beginning of the 6th century BC, were metallographically analysed (Török et al. 2024). These samples show great similarity to the here analysed, both in weight (around 1, 54 kg a piece) and the processing level - they were defined as very well compacted, standing somewhere between bloom and a bar. This is completely in line with results obtained by simple density measurement within this research, by which the bloom can be defined as a heavily purified bloom, reheated and consolidated by wooden hammer to a maximum achievable level. The use of an iron hammer in interpretation of such archaeological objects cannot of course be excluded, however, the structure of the outer surface of the sample does not imply such treatment. The sample is only a part of the original bloom, and represents approximately one sixth of the original bloom and exhibits cutting surfaces on two sides. Multiple sectioning of a bloom of this size would have required substantial reheating, which may explain the comparatively advanced reheating stage observed. This reheating stage can thus be interpreted as a technological requirement for subdividing an initially large bloom into smaller, more manageable semi-products intended for further processing. Comparable morphologies have been documented in metallographically analysed semi-products (Török et al. 2024, Fig. 2: 1, 46).

The Early Medieval samples from Somogyfajsz (Table 4: 10–12) fall within the range of uncompacted iron sponges to compacted iron blooms. The shape of the blooms and their surface texture suggest a low degree of compaction. This limited treatment is consistent with the archaeological context, as the blooms were found together directly in front of a smelting furnace embedded in the wall of a working pit at the iron-smelting site in Somogyfajsz (Gömöri, pp. 153–164, Fig. 112). The samples exhibit pronounced differences in volume and size (Fig. 10) and minor differences in density and mass. However, normalisation to estimated metallic iron mass (Table 4: $m_{\text{metallic iron}}$), reveals pronounced similarity in metallic iron yield among the blooms. This pattern may indicate a marked uniformity in smelting output—primarily reflecting the amount of ore charged into the furnace—accompanied by only limited variation in post-reduction processing

The half-bloom sample from the Pusztakovácsi site (Table 4: 9), potentially dating to the same period as the nearby Somogyfajsz site samples (Somogy County, Hungary), exhibits a somewhat higher degree of purification yet ultimately yields a very similar estimated mass of metallic iron. As the specimen represents only half of a single bloom, the original bloom would be expected to have contained approximately twice the iron content. Although the precise chronological relationship between the Somogyfajsz and Pusztakovácsi samples remains uncertain, if these semi-products were in circulation contemporaneously, the observed pattern could indicate variability in smelting outcomes alongside standardisation of semi-products through post-reduction processing. Such standardisation could have been achieved by regulating weight (not size or level of postreduction processing), that is, by controlling the content of forgeable iron within semi-products intended for further distribution. Variability in smelting outcomes may reflect either technological choices made by individual workshops or factors that were difficult to control, such as the quality of the ores used. This interpretation is consistent with the generally variable quality of bog iron ores, the type of ore exploited in Somogy County during the Early Middle Ages (Gömöri 2000). The bog ores exhibit naturally variable iron–gangue ratios and may therefore condition differing smelting efficiencies even under similar operational parameters. This interpretation is supported by experimental smelting studies conducted on bog iron ores from the same production region, those in Somogy County, Hungary, and the Podravina region in Croatia (Karavidović 2020; Karavidović, Brenko 2022) as well as analysis of ores from Early Medieval archaeological contexts in the Podravina region (Brenko et al. 2021).

Table 4 Measured (weight, density) and estimated (Fe%, $m_{metallic\ iron}$ and P%) values for archaeological iron semi-products, based on a review of the literature and available archaeological finds.

4. Táblázat: Régészeti vasbucákra meghatározott sűrűség adatok (irodalmi adatokkal kiegészítve) és ez alapján a becsült vastartalom (Fe%), a bennük lévő tiszta fémes vas tömege ($m_{metallic\ iron}$) és porozitásuk (P%)

Sample	Site	m (kg)	ρ (g/cm³)	Fe (%)	$m_{metallic\ iron}$ (kg)	P (%)	Period*	Datation	Context	Note	Bibliography
		measured		calculated							
1	Klášťov 1**	0,72	4,01	63,9	0,46	26,1	EM	8-9th century	Moravia, CZ (Vysoké Pole–Klášťov) - early medieval sacral place or a hilltop settlement. Blooms found in hoards via. metal detector prospecting.	half	Merta 2019
2	Klášťov 2**	0,95	5,75	79,9	0,76	8,6				half	
3	Klášťov 3**	1,03	4,47	68,1	0,70	20,6				half	
4	Klášťov 4**	3,10	4,49	68,3	2,12	20,4				complete	
5	Klášťov 5**	1,66	3,69	60,9	1,01	30,3				half	
6	Staré zámky u Líšně**	1,45	4,69	70,1	1,02	18,2			Moravia, CZ - hillfort settlement. Blooms found outside the rampart of the outer bailey of the hillfort, via metal detector prospecting. The site is considered a place from which iron production in the nearby smelting centre in the central part of the Moravian Karst was organised (Olomučany), and to which the output of the smelting workshops most likely flowed.	half(?); estimated total weight 2,2-2,3 kg	
7	Olomučany I**	2,15	3,91	63,0	1,36	27,4			Moravia, CZ. Iron production site (98/1). Blooms (2x) found burried in front of a smelting furnace.	complete	
8	Labod-Petesmalom***	9,55	5,03	73,3	7,00	14,8			Somogy county, HU. Surface find near an excavated iron production site.	wedged	Gömöri 2000; 2018; Török et al. 2017; 2018
9	Pusztakovacsi***	1,97	4,28	66,4	1,31	22,8		10th-11th century	Somogy county, HU. Surface find near smelting slag surface finds. Area close to the Somogyfajsz smelting site and in contextual relation (Gomori 2000: 164, 138).	half	unpublished, Ripl Rónai Museum, Kaposvár, Hungary; site registered: Gomori 2000:138
10	Somogyfajsz***	2,45	3,33	57,6	1,41	35,3		middle - end of 10th century	Somogy county, HU. Iron production site - working pit no. 1 , found in front of the smelting furnace no.6. Workspace dated to middle to end of 10th century.	complete	Gömöri 2000:153-164, fig. 112;2006; 2018; Pleiner 2000
11	Somogyfajsz***	2,41	3,97	63,5	1,53	26,6				complete	
12	Somogyfajsz***	2,00	4,18	65,5	1,31	24,0				complete	
13	Jakab-hegy (394/8)***	2,43	3,41	58,4	1,42	34,2	EIA-LIA	9th - 6th or 3rd-1st century BC (?)	Baranya county, HU. Shallow pit deposit , hoard (29 blooms) associated with multi-period site - Early Iron Age settlement snd burial mounds (Ha C/D) or La Tene (Lt C/D).	complete	unpublished, Janus Pannonius Museum, Pécs, Hungary
14	Jakab-hegy(394/16)***	2,36	4,03	64,1	1,51	25,8				complete	
15	Jakab-hegy(394/15)***	3,59	3,82	62,1	2,23	28,5				complete	
16	Jakab-hegy(394/6)***	3,46	3,93	63,2	2,19	27,1				complete	
17	Jakab-hegy (394/22)***	2,50	4,75	70,7	1,76	17,6				complete	
18	Verebce-bérc***	1,29	5,91	81,4	1,05	7,5	EIA	end of the 7th century – beginning of the 6th century BC (?)	Bükk Mountains, HU. Surface find, hoard found in 2007 in the area of Early Iron Age hillfort settlement Dédestapolcsány-Verebce-bérc.	slice (two cut surfaces), 1/6 of initial bloom	Finds: Török et al.2011. Reference to the site: Szabó et al. 2022, Török et al.2024

*EM - Early Medieval Period; EIA - Early Iron Age; LIA - Late Iron Age

** weight and density present in primary publication

***measured in this research

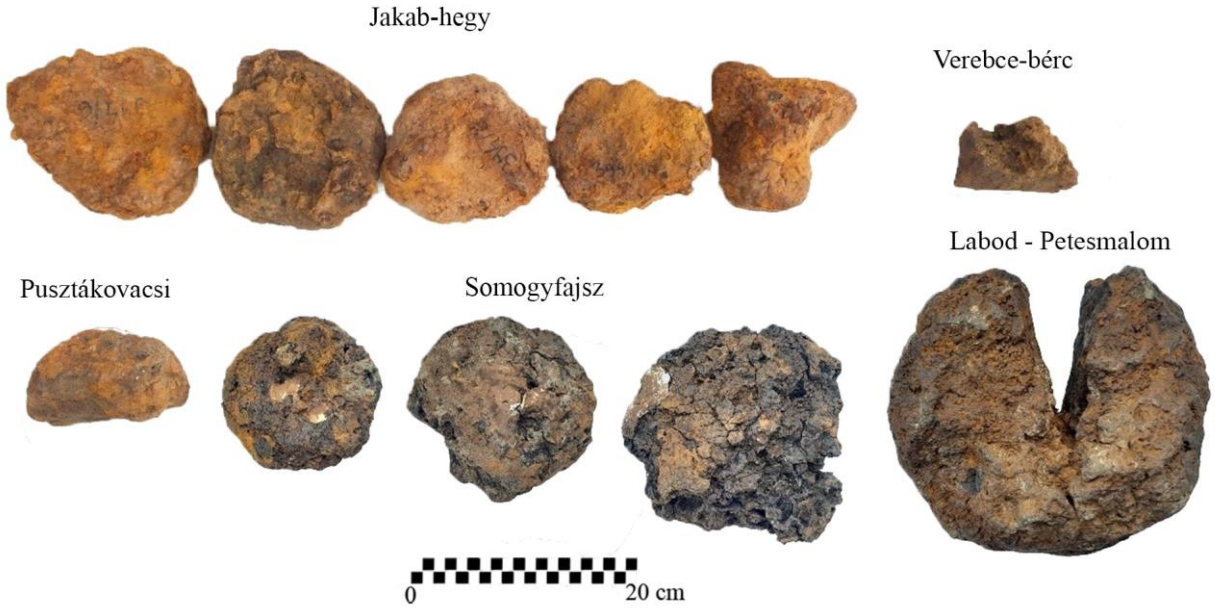

Figure 10 Samples of iron blooms from archaeological context dated to Iron age and Early Medieval period, measured for density.
10. Ábra: Sűrűségmérésbe bevont régészeti vasbucák (vaskoriak és középkoriak)

4. Discussion – Applicability and Limitations of the Proposed Models

The establishment of characteristic density ranges for varying degrees of refinement provides a valuable means of inferring technological practices employed in the production of iron semi-products. The density measurement can be achieved through a straightforward, simple and non-destructive measurement method based on water displacement (the Archimedes principle), highly applicable on any archaeological find or alternatively through volume calculation via 3D modelling. If combined with more commonly used analytical approaches, such as visual inspection and/or metallographic analysis of iron semi-products (Bauvais, Fluzin 2009; Galili et al. 2015; Merta 2019; Saage et al. 2018; Török et al. 2018, 2022, 2024; Strobl et al. 2010; Souchopova, Stransky 1999), they could yield comprehensive insights into the technology of iron semi-product production.

However, it must be emphasised that in cases involving lower levels of refinement, the proposed density thresholds should be regarded as somewhat variable. This is particularly evident at the transitional boundaries between the uncompacted and compacted, and heavily compacted and reheated bloom states. Such potential variation is linked to differences in ore composition, smelting parameters, and post-smelting handling - predictively variable within different archaeological contexts. The nature of the ore (primarily quality in terms of iron to gangue ratio) and the smelting process parameters can influence the formation, structural coherence and initial density of the sponge iron, which in turn affects the subsequent efficiency of compaction. Furthermore, the latter can be influenced by the rate at which hammering is applied within the limited timeframe during which the iron sponge remains sufficiently hot and malleable following extraction from the smelting furnace. A higher hammering rate, potentially achievable through the coordinated efforts of multiple smiths—as opposed to the single-person operation employed in experimental reconstructions—could improve compaction efficiency.

Nevertheless, this potential variability should be considered limited to the borderline values of the proposed density ranges, as each stage of the technological process is inherently constrained by practical and material limitations. For instance, a denser iron sponge—resulting from lower slag inclusion—would typically be less coherent structurally, more brittle, and less malleable, increasing the risk of fragmentation during compaction. It would also cool more rapidly than slag-rich sponge, reducing the window for effective forging and limiting the degree of consolidation achievable without reheating. This practical constraint highlights the ethnographically, historically and morphologically documented use of wooden hammers and softer surfaces (wooden log as an anvil) during the initial stages of bloom refinement (Pleiner 2000). Given the fragility of the bloom upon removal from the smelting furnace, the application of a wooden hammer allows for a gentler, more controlled compaction, thereby reducing the risk of damage and limiting the force and rate of hammering. This, in turn, defines the maximum density attainable prior to reheating, around 5 g/cm^3 according to experimental testing. Likewise, the density attainable using a wooden hammer, even during repeated

reheating, is limited by its low force transmission, which prevents the expulsion of finer slag and the reduction of smaller internal voids. Archaeological evidence of wooden hammer and a form of anvil made of wood (for instance a log) use is observable in surface texture characteristics and shape of the vast majority of blooms, and the overall density ranges of analysed experimental blooms support the conclusion that significant reduction in porosity and moderate levels of purification—up to approximately 6 g/cm³ (c. 82% iron, 5 % porosity)—could be achieved using wooden hammers and base surface such as wood during reheating and refinement. The majority of published and examined archaeological blooms from across Europe—irrespective of chronological period, geographic region, or cultural context—exhibit densities between 3.5 and 6 g/cm³ (Pleiner 2000; 2003; Merta 2019; Espelund 2000; Dungworth 2015). These values are consistent with the density range observed in experimental material (Table 1,2) and case study archaeological samples (Table 5), extending from unprocessed iron sponge through to compacted and, ultimately, blooms heavily refined with wooden hammer - implicating applicability of the classification model. The boundary density value of around maximum of 6g/cm^3 achieved by wooden hammer corresponds quite well with archaeological data, implicating similar mechanical constraints in archaeological records i.e. an applicable boundary condition.

The model for calculating iron content based on density (Eq. 4), derived from the purification of both experimentally produced blooms and an archaeological sample, yielded an approximation with a high coefficient of determination ($R^2 \approx 0{,}95$), indicating strong model reliability and predictive accuracy by explaining the vast majority of the variability observed. Quantification of iron and porosity from digital cross-section surface analysis of semi-products at different stages of refinement falls within the compositional ranges for iron sponges, blooms, and bars estimated by Equation 4, thereby providing independent validation of the density-based model. Image-based cross-section measurements offer an alternative approach for estimating iron, slag, and porosity contents; however, given the inherent heterogeneity of phase distribution within blooms, reliable results can only be obtained when a complete cross-section of the object is analysed. Small samples, typical of metallographic examination, may therefore yield biased results due to localised compositional heterogeneity. If used as a standard comparative reference, the bulk semi-product density-based model offers a valuable tool for archaeometallurgical studies. However, it should be noted that the model is somewhat limited. For greater accuracy, it would be worthwhile to determine the correlation (Eq. 4) separately for different size/weight and density ranges on multiple samples. As is, the proposed model demonstrates very good predictive accuracy and is best suited for application to archaeological finds of iron sponges and blooms weighing between 1 and 5 kg, with densities ranging from 3-6 g/cm^3, as well as more heavily purified semi-products with densities reaching nearly the pure iron density up to approx. 7,7 g/cm^3. The model may be extended to heavier blooms, as a standard comparative reference, bearing in mind that a slight underestimation of iron content is possible.

The correlation of the model with archaeological samples is further supported by the inclusion of one archaeological bloom in the experimental forging (Table 2: 6*, Figure 7). The basic structural characteristics (relative slag and porosity ratio), present in the cross-section of the sample, are quite similar to refinement category presumed by density measurement, the compacted blooms. However, among experimentally forged samples, the archaeological specimen exhibits the greatest mass loss per unit of density increase between the initial compacted bloom stage and the final forged bar (Figure 9a: 6 and 6*, Table 3). The somewhat higher mass loss per density observed in the archaeological sample may reflect its different state of preservation relative to the experimentally produced blooms. While the sample still exhibits typical characteristics of bloomery iron semi-product, classified here as compacted, its surface is affected by a stratified corrosion layer, and internal corrosion may have weakened its structural integrity. The corrosion layer on buried archaeological iron artefacts, as observed on the outer surface of the sample (Figure 5), typically consists of goethite (α-FeO(OH)), magnetite (Fe_3O_4), lepidocrocite (γ-FeOOH), and maghemite (Fe_2O_3) minerals (Neff et al. 2005; Pons 2002). In many archaeological contexts, burial deposits such as clay, sand, and other mineral particles become embedded within the corrosion layer (Neff et al. 2005). All of these minerals have densities lower than the metallic iron – the iron oxy(hydroxide)s between 3,3-4,3 g/cm^3 (goethite) and 4,9-5,7 g/cm^3 (magnetite) and other even lower in the case of clayey and sandy minerals (Anthony et al. 2016). The presence of this composite corrosion layer may therefore alter both the measured mass and volume of the bloom, resulting in a lower apparent density when treated as a three-phase material (metallic iron, slag, air). During purification, corroded and structurally weakened areas are prone to cracking and flaking. As a consequence, both non-metallic corrosion products and structurally compromised metallic iron may be lost more readily (burn-off), contributing to elevated mass loss values. Accordingly, the mass loss relative to density increase is

somewhat higher than that observed in experimental samples, where surface corrosion is absent and structure is more stable (Table 3: 6*). Nevertheless, the mass loss percentage value of the archaeological bloom (Table 3) falls within the broader range defined for compacted blooms refined into bars with a density of approximately 7,5 g/cm^3 (21-40%). When compared directly with an experimental sample of similar initial density (Table 3: Sample 1 vs. Sample 6*), the higher burn-off loss of the archaeological specimen may also be partially attributed to differences in initial mass. Larger blooms (as experimental sample 1) tend to exhibit lower proportional metallic iron losses owing to a smaller specific surface area exposed during forging. This size/mass-dependent effect, should be understood as universal, applicable to both experimental and archaeological material. Taken together, the data indicate that experimentally produced samples can replicate structural or compositional characteristics observed in the archaeological bloom, such as high initial slag content, refinement level, or comparable microstructural porosity. It also implies that post-depositional changes do not significantly alter the bloom's properties, allowing for a high degree of agreement and comparability.

Limited variability should be expected in estimation of the mass of semi-product at any given density (Eq. 5) and the metallic iron mass of an archaeological object. These values in principle reflect the yield attainable under historically plausible post-reduction conditions. In the experimental purification of blooms into bars, a power hammer was employed, allowing for short forging cycles (4–5 reheats) and minimal iron loss through burn-off, taken as a boundary state for further calculation. However, the power hammer simulates the output of two or three highly skilled smiths working in unison. If, instead, production involved a single smith or a less skilled team, the number of reheats required would likely increase due to limited deformation and slag expulsion per cycle, resulting in greater burn-off iron losses. This factor remains difficult to quantify experimentally and is subject to variation between individual archaeological contexts. While experimental quantification can provide generalised standards—such as estimates of metallic iron yield mass ($m_{metallic\ iron}$), iron content (Fe%) or mass of a semi-product at any given density ($m_{semi\text{-}product}$)—it cannot yield precise predictions and account for the inherent variability of past production conditions, shaped by latent and often unquantifiable factors such as the number of smiths, their skill level, and specific working practices.

5. Conclusion

The experimental testing of post-reduction techniques of refinement yielded a stage-based classification system, based on density measurement, that can be applied reliably to archaeological iron semi-products. Since the density of an iron semi product reflects its internal structure, including porosity and slag inclusion, it can be used to calculate the percentage of iron (Fe%) and metallic iron content ($m_{metallic\ iron}$) within a given semi-product as well as potential mass of a semi-product at any given density (m_{sp}).

The predictive models for stage-based classification and calculation of iron content can be taken as proxies for evaluation of some key archaeological questions:

1. Degree of refinement and techniques applied:

Different types of iron semi-products may have varying densities depending on post reduction refinement characteristics. Based on comparative experimental data these can inform of technique, degree of refinement and forgeable iron content: (1) ρ = 3–4 g/cm³ – uncompacted iron sponge, product of direct reduction, containing between 55% and 64% of forgeable iron; (2) ρ = 3,5–5 g/cm³ – compacted iron bloom, hammered with wooden tools while hot (subsequent to extraction from the smelting furnace), containing between 59% and 73% of forgeable iron; (3) ρ = 5–6 g/cm³ – reheated and purified bloom, using wooden hammer on a wooden anvil, containing 73–82% of forgeable iron; (4) $\rho \approx$ 7,3–7,7 g/cm³ –-iron bar, further reheated and hammered with iron hammer on an iron anvil, containing ca. 93–98% of iron**.** The density of an object increases in correlation with the degree of purification achieved during the refining process, ultimately approaching—but remaining slightly below—the density of pure iron (7,87 g/cm³) in the case of iron bars. Densities over 6 – $\approx$ 7,3 g/cm^3 can be regarded as heavily refined (iron hammer and anvil) iron blooms or bars, depending on other morphological factors, containing between 82 and 93% of iron.

For archaeological samples, density measurements may be slightly affected—typically lowered—by corrosion, especially if untreated. However, analysis of experimentally forged bloom from archaeological context indicates that these discrepancies are not highly altering and align well within established predictive models. As a result, predictive modelling of both density and iron content remains valid and applicable.

2. Technological efficiency and quantification of iron produced:

Density data, when combined with experimentally derived iron content prediction (Fe%=9,24ρ + 27,2), allow for estimation of mass of the semi product at any density, ranging from the uncompacted iron sponge through

postreduction processing to an iron bar ($m_{semi-product} = m_0 \frac{9{,}24\rho_0+27{,}2}{9{,}24\rho+27{,}2}$). This, in turn, can inform further reconstructions of post-reduction and even reduction efficiency and resource management (e.g. ore-to-metal ratio) as well as quantification of total iron available for further processing.

3. Functional assessment and comparative analisys:

The density of iron semi-products (e.g. sponge, compacted or consolidated bloom, bar) varies according to their stage of refinement in the *chaîne opératoire*. If degree of purification is taken as a technological choice, it may reflect the intended function of an object. Calculating density and iron content can help identify functional standards and support comparative studies across sites and timeframes, revealing technological choices, cultural practices, socio-economic conditions, and resource management.

4. Non-destructive evaluation:

Especially when obtained via Archimedes principle, 3D scanning or gas pycnometry in combination with water displacement, density offers a non-invasive method to assess internal integrity and gain additional information about the object, without cutting or sampling rare or fragile artefacts.

Application of density measurement and iron content calculation transforms iron semi-products from descriptive typologies into quantifiable technological indicators. It bridges the gap between material remains and the decisions, knowledge, tradition and evolution as well as constraints that shaped past metallurgical practices.

Acknowledgements

This work was supported by the Croatian Science Foundation through the project Cultural Landscapes of Iron Metallurgy During Antiquity and the Early Middle Ages in the Sava and Drava River Basin – KulturFER [IP-2022-10-1846].

Bibliography

ANTHONY, J. W., BIDEAUX, R. A., BLADH, K. W. & NICHOLS, M. C. (2016): Handbook of mineralogy. Mineralogical Society of America, Chantilly, VA, USA. http://www.handbookofmineralogy.org/, accessed 20.07.2025.

BAUVAIS, S. & FLUZIN, P. (2009): Archaeological and archeometrical approaches of the chaîne opératoire in iron and steelmaking: methodology for a regional evolution study. In: ROUX, V. & ROSEN, S. (eds.), *Techniques and people: anthropological perspectives on technology in the archaeology of the proto-historic and early historic periods in the southern Levant*, 157–178. Paris: De Boccard.

BERRANGER, M. & FLUZIN, P. (2011): From raw iron to semi-product: quality and circulation of materials during the Iron Age in France. *Archaeometry* 54(4): 664–684. https://doi.org/10.1111/j.1475-4754.2011.00641.x

BIELENIN, K. (1977): Einige Bemerkungen über das altertümliche Eisenhüttenwesen im Burgenland. Wissenschaftliche Arbeiten aus dem Burgenland 59: 49–62.

BRENKO, T., BOROJEVIĆ ŠOSTARIĆ, S., RUŽIČIĆ, S. & SEKELJ IVANČAN, T. (2020): Evidence for the formation of bog iron ore in soils of the Podravina region, NE Croatia: geochemical and mineralogical study. *Quaternary International* 536: 13–29. https://doi.org/10.1016/j.quaint.2019.11.033

BRENKO, T., BOROJEVIĆ ŠOSTARIĆ, S., KARAVIDOVIĆ, T., RUŽIČIĆ, S. & SEKELJ IVANČAN, T. (2021): Geochemical and mineralogical correlations between the bog iron ores and roasted iron ores of the Podravina region, Croatia. *Catena* 204: 105353. https://doi.org/10.1016/j.catena.2021.105353

BUCHWALD, V. F. (2005): Iron and steel in ancient times. Historisk-filosofiske Skrifter 29. The Royal Danish Academy of Sciences and Letters, Copenhagen, 352 pp.

CREW, P. (1991): The experimental production of prehistoric bar iron, *Journal of the Historical Metallurgy Society* 25: 21–36.

CREW, P. & CREW, S. (1994): The experimental production of bar iron. In: MANGIN, M. (ed.), *La sidérurgie ancienne de l'Est de la France dans son contexte européen* (Besançon conference 1993): 175–176.

DILLMANN, P., FLUZIN, P. & URTEAGA, M. (1997): Refining of an experimental Biscaian bloom from Agorregi. In: CREW, P. & CREW, S. (eds.), *Early ironworking in Europe: archaeology and experiment. Abstracts of an international conference symposium, Plas Tan y Bwlch, 19–25 September 1997*, 73–75. Maentwrog: Plas Tan y Bwlch, Snowdonia National Park Study Centre.**DUNGWORTH, D.** (2015): Iron bloom. In: ATKINSON, M. & PRESTON, S. J. *Heybridge: A Late Iron Age and Roman settlement, Excavations at Elms Farm 1993–5*. Internet Archaeology 40. http://dx.doi.org/10.11141/ia.40.1.dungworth1

ESCHENLOHR, L. & SEERNELS, V. (1991): Les bas fourneaux mérovingiens de Boécourt, Les Boulies (JU/Suisse). *Cahier de archéologie jurassienne* 3. Porrentruy: Office du Patrimoine Historique, Société Jurassienne d'Émulation.

ESPELUND, A. (2013): The evidence and the secrets of ancient bloomery ironmaking in Norway – with an extension to the beginning of the industrial period. Trondheim: Arketype Forlag, 319 pp.

GALILI, E., BAUVAIS, S., ROSEN, B. & DILLMANN, P. (2015): Cargoes of iron semi-products recovered from shipwrecks off the Carmel coast, Israel. *Archaeometry* 57(3): 505–535. https://doi.org/10.1111/arcm.12077

GÖMÖRI, J. (2000): Az avar kori és Árpád-kori vaskohászat régészeti emlékei Pannoniában: Magyarország iparrégészeti lelőhelykatasztere I. Vasművesség / The archaeometallurgical sites in Pannonia from the Avar and early Árpád period: register of industrial sites in Hungary 1. Ironworking. Sopron: Soproni Múzeum.

GÖMÖRI, J. (2018): Technológia-kontinuitási kérdések a somogyi vasvidék „izzó" vasbucái fényében / Questions of technological continuity in the light of the glowing iron blooms found on sites in county Somogy. In: VARGA, M. & SZENTPÉTERI, J. (eds.):

Két világ határán. Természet- és társadalomtudományi tanulmányok a 70 éves Költő László tiszteletére. Kaposvár: A Kaposvári Rippl-Rónai Múzeum Közleményei 6, 77–87.
JOOSTEN, I., JANSEN, J. & KARS, H. (1998): Geochemistry and the past: estimation of the output of a Germanic iron production site in the Netherlands. *Journal of Geochemical Exploration* 62: 129–137.
KARAVIDOVIĆ, T. (2020): Močvarna željezna ruda – eksperimentalno testiranje utjecaja prženja rude na postupak taljenja i krajnji proizvod / Bog iron ore – experimental testing of the impact of ore roasting on the smelting process and the end product. *Annales Instituti Archaeologici* XVI/1: 143–152.
KARAVIDOVIĆ, T. & BRENKO, T. (2022): Nature of the deposit and properties of bog iron ore at the Kalinovac – Hrastova Greda. Prilozi Instituta za arheologiju u Zagrebu 39(2): 219–261. https://doi.org/10.33254/piaz.39.2.5
KERBLER, L. J. & KREINZ, A. (2013): Ein frühmittelalterlicher Eisenverhüttungsplatz in Dörfl, Burgenland. Beiträge zur Mittelalterarchäologie in Österreich 29 (Nearchos Sonderheft 20): 105–114.
KERCSMÁR, Zs. & THIELE, Á. (2015): A belső-somogyi gyepvasércek genetikája és geokémiai jellemzői, földtani és archeometallurgiai megközelítés alapján / Genetic types and geochemistry of bog iron ore deposits from Inner Somogy, from a geological and archaeometallurgical perspective. *Földtani Közlöny* 142(1): 53–71.
MEHOFER, M. (2010): Archäologische und technologische Untersuchungen zur Eisenverhüttung und Verarbeitung in der awarischen Siedlung von Zillingtal/Burgenland. In: HEROLD, H. (ed.), Die awarische Siedlung von Zillingtal 80/2, 207–234. Eisenstadt.
MERTA, O. (2019): Známé nálezy raně středověkých železářských naseknutých lup z území Moravy. *Archeologia Technica* 30: 4–13.
NEFF, D., DILLMANN, P., BELLOT-GURLET, L. & BERANGER, G. (2005): Corrosion of iron archaeological artefacts in soil: characterisation of the corrosion system. *Corrosion Science* 47: 515–535. https://doi.org/10.1016/j.corsci.2004.05.029
PLEINER, R. (2000): Iron in archaeology: the European bloomery smelters. Praha: Archeologický ústav AV ČR, xviii + 400 pp.
PLEINER, R. (2003): European iron blooms. In: NORBACH, L. (ed.): *Prehistoric and medieval direct iron smelting in Scandinavia and Europe: aspects of technology and science.* Aarhus University Press, Aarhus, 183–189, 305–307.
PLEINER, R. (2006): *Iron in archaeology: early European blacksmiths*. Praha: Archeologický ústav AV ČR.
PONS, E. (2002): Long term corrosion of iron and non-alloy or low-alloy steels in clay soils: physico-chemical characterisation and electrochemical study of archaeological analogues. Université de Technologie de Compiègne, Laboratoire Roberval (France). Unpublished PhD thesis.
SAAGE, R., PEETS, J., KULU, P., PEETSALU, P. & VILJUS, M. (2018): Metallographic investigation of iron blooms and bars from the smithy site of Käku, Estonia. *Fennoscandia Archaeologica* XXXIV: 46–58.
SEKELJ IVANČAN, T. & KARAVIDOVIĆ, T. (2021): Archaeological record of iron metallurgy along the Drava River. In: SEKELJ IVANČAN, T. & KARAVIDOVIĆ, T. (eds.): *Interdisciplinary research into iron metallurgy along the Drava River in Croatia – The Transfer project.* Oxford: Archaeopress Publishing Ltd., 43–91. http://doi.org/10.32028/9781803271026-4
SENN, M., GFELLER, U., GUÉNETTE–BECK, B., LIENEMANN, P. & ULRICH, A. (2010): Tools to qualify experiments with bloomery furnaces. *Archaeometry* 52(1): 131–145. https://doi.org/10.1111/j.1475-4754.2009.00461.x
STROBL, S., HAUBNER, R. & KLEMM, S. (2010): Metallographic investigations of a historical bloom found in Styria – Austria. In: LONGAUEROVA, M. (ed.), *Acta Metallurgica Slovaca Conference, Special Issue, 14th International Symposium on Metallography* 1: 655–660.
SOUCHOPOVÁ V., STRÁNSKÝ, K. (1999): Raněstředověké středoevropské polotovary železa, *Archeologia technica* 11: 22–30.
SOUCHOPOVÁ, V. (1986): Hutnictví železa v 8.–11. století na západní Moravě. Studie Archeologického ústavu Československé akademie věd v Brně XIII/1. Praha: Academia.
SZABÓ, G. V., BARCSI, M., BÍRÓ, P., TANKÓ, K., VÁCZI, G. & MOGYORÓS, P. (2022): Investigations of an Early Iron Age siege. Preliminary report on the archaeological research carried out at Dédestapolcsány–Verebce-bérc between 2020 and 2022. *Dissertationes Archaeologicae ex Instituto Archaeologico Universitatis de Rolando Eötvös Nominatae*, Ser. 3, 10: 277–299. https://doi.org/10.17204/dissarch.2022.277.
THIELE, Á. & TÖRÖK, B. (2011): Vastermelés, vaskihozatal és a kohósított gyepvasércek minimálisan szükséges vastartalma az avar és Árpád-kori vasbucakohászatban. Archeometriai Műhely 4: 345–350.
TÖRÖK, B., BARKÓCZY, P., KOVÁCS, Á., KÖLTŐ, L., FEHÉR, A. & SZŐKE, M. B. (2018): Pannóniai kora középkori ékelt vasbucák összehasonlító archeometriai vizsgálata. *Bányászati és Kohászati Lapok, Kohászat*, Budapest 151(3): 1–4.
TÖRÖK, B., BARKÓCZY, P. & SZABÓ, G. (2022): First archaeometrical approach to the examination of Iron Age ferrous fragments from Regöly and Bükkábrány (Hungary): the inception of iron working in the Carpathian Basin? *Interdisciplinaria Archaeologica – Natural Sciences in Archaeology* XIII/2: 143–154.
TÖRÖK, B., KOVÁCS, A., BARKÓCZY, P., KÖLTŐ, L., FEHÉR, A. & SZŐKE, B. M. (2017): A complex comparative study of early medieval split blooms from Pannonia. International Conference *Iron in Archaeology, Bloomery Smelters and Blacksmiths in Europe and Beyond*, Prague, 30 May–1 June 2017, poster presentation.
TÖRÖK, B., BARKÓCZY, P. & SZABÓ, G. (2024): Huge amounts of iron raw material from the Early Iron Age settlement of Dédestapolcsány-Verebce (N-Hungary) – a preliminary archaeometallurgical study. *Archeometriai Műhely*, 285–294. https://doi.org/10.55023/issn.1786-271X.2024-023
TÖRÖK, B., KOVÁCS, Á., P., FISCHL, K., BARTHA, ZS., THIELE, Á. (2011): Vasdepók problémája Mályinka-Verebce bércen, *Archaeometriai Ankét*, Budapest, Hungary, poster presentation.https://www.bucavasgyuro.net/data/publikaciok/Poszter+rovidcikk/Poszter_AA2011.jpg. Accesed 20.07.2025
TYLECOTE, R. F., AUSTIN, J. N. & WRAIGHT, A. E. (1971): The mechanism of the bloomery process in shaft furnace. *Journal of the Iron and Steel Institute* 209: 342–363.

Declarations

- The manuscript is original, not published previously, and not under consideration elsewhere.
- All authors have approved the final version and consent to submission.
- Conflicts of interest: none declared.
- Funding: Croatian Science Foundation through the project Cultural Landscapes of Iron Metallurgy During Antiquity and the Early Middle Ages in the Sava and Drava River Basin – KulturFER [IP-2022-10-1846].
- Ethical approval: not applicable (no human or animal subjects).